Turkish J. Eng. Env. Sci.
27 (2003) , 361 – 373.

Active Control of Seat Vibrations of a Vehicle Model Using Various Suspension Alternatives

Rahmi GÜÇLÜ
Yıldız Technical University, Faculty of Mechanical Engineering,
İstanbul-TURKEY
e-mail: guclu@yildiz.edu.tr

Received 12.10.2001

Abstract

The dynamic behavior of a non-linear 8 degrees of freedom vehicle model having active suspensions and a PID controlled passenger seat is examined. The non-linearity occurs due to dry friction on the dampers. The suspensions are considered as McPherson strut-type independent suspensions. Three cases of control strategies are taken into account. In the first case, only the passenger seat is controlled. In the second case, only the vehicle body is controlled. In the third case, both the vehicle body and the passenger seat are controlled at the same time. Since the PID control method can be applied easily and is well known, it has an important place in control applications. The time responses of the non-linear vehicle model due to road disturbance and the frequency responses of the harmonically linearised non-linear vehicle model are obtained for each control strategy. At the end, the performances of these strategies are compared and discussed.

Key words: PID control, Vehicle model, Active suspensions.

Introduction

Vehicle suspension can be treated as a dynamic system using vehicle properties and simulating the response of the vehicle to various inputs and disturbances. Suspension serves the basic function of isolating passengers and the chassis from the roughness of the road to provide a more comfortable ride. Due to developments in the control technology, electronically controlled suspensions have gained more interest. These suspensions have active components controlled by a microprocessor. By using this arrangement, significant achievements in vehicle response can be carried out. Selection of the control method is also important during the design process. In this study PID controllers parallel to McPherson strut-type independent suspensions are used. The major advantages of this control method are its relative simplicity in design and the availability of well-known standard hardware. To simplify models, a number of researchers assumed vehicle models to be linear. However, such models contain non-linearities that should be taken into account. By including non-linearities such as dry friction on dampers, the results become more realistic.

In the last decade many researchers applied some linear and non-linear control methods to vehicle models. Because of simplicity, quarter car models were mostly preferred. Redfield and Karnopp (1988) examined the optimal performance comparisons of variable component suspensions on a quarter car model. Yue *et al.* (1989) applied some linear control methods to a quarter car model. Stein and Ballo (1991) designed a passenger seat for off-road vehicles with active suspensions. Hac (1992) applied optimal linear preview control on the active suspensions of a quarter car model. Rakheja *et al.* (1994) added a passenger seat in their analysis. A passenger seat suspension system was described by a generalized 2 degrees of freedom model and with non-linearities such as shock absorber damping, linkage friction and bump stops. Since the quarter car

model is insufficient to give information about the angular motions of a vehicle, some researchers used more complex models like half and full car models. These models give information about the pitch, roll and bounce motions of a vehicle body. Crolla and Abdel Hady (1991) compared some active suspension control methods on a full car model. Integrated or filtered white noise was taken as the road input. The same researchers applied linear optimal control law to a similar model in 1992. Hrovat (1993) compared the performances of active and passive suspension systems on quarter, half and full car models using optimal control laws. Dry friction on dampers is one of the main factors affecting ride comfort. On good road surfaces and at low vehicle speeds, the effect of road input cannot overcome dry friction force and, therefore, the suspensions are almost locked, which is known as Boulevard Jerk, and an uncomfortable vibration mode becomes effective due to reduced degrees of freedom (Silvester, 1966). Some applications using non-linearity on active suspensions were achieved. Alleyne *et al.* (1993) compared sliding mode controlled active suspensions with PID controlled active suspensions. Yagiz *et al.* (2000) applied sliding mode controlled active suspensions to a linear 7 degrees of freedom vehicle model.

A study has been carried out for linear motors where a satisfactory response to PID controllers can be obtained (Otten *et al.*, 1997). The operating principle of the linear motor is shown in Figure 1. It is composed of 2 main parts. These are a number of base-mounted permanent magnets forming the stator and a translator formed by a number of iron-core coils. By applying a 3-phase current to 3 adjoining coils of the translator, a sequence of attracting and repelling forces between the poles and the permanent magnets is generated. This results in a thrust force experienced by the translator. The motor is a synchronous, permanent-magnet motor with electronic commutation.

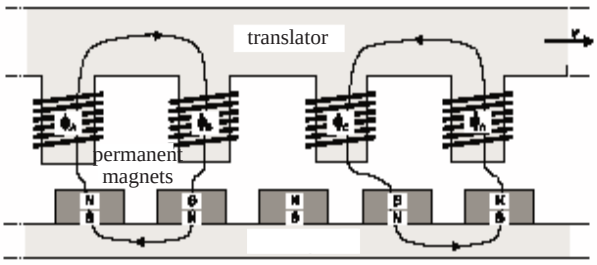

Figure 1. Operating principle of a linear motor.

In this study, the aim is to compare some control strategies applied on the purely linear and harmonically linearized non-linear full car model in order to obtain ride comfort using a PID control. A passenger seat is included in the vehicle model so that the response of the passenger due to a road disturbance can be observed. There are 3 strategies that have been taken into account. The first strategy includes conventional suspensions and a controlled passenger seat. In the second strategy, the model has active suspensions and a normal passenger seat. The last model is fully controlled, i.e. both the suspensions and passenger seat have controllers.

Vehicle Model

The non-linear full car model used in this study is shown in Figure 2. It includes all possible control strategies. This full car model has 8 degrees of freedom, namely x_1, x_2, x_3, x_4, x_5, x_6, $x_7 = \theta$ and $x_8 = \alpha$. These are the motion of the right front axle, the motion of the left front axle, the motion of the right rear axle, the motion of the left rear axle, the bounce motion of the passenger seat, the bounce motion of the vehicle body, the pitch motion of the vehicle body and the roll motion of the vehicle body, respectively. The aim is to improve the ride comfort of the passengers. The common application in modeling the vehicle with a passenger seat is to add only 1 passenger seat preferably in the driver seat position (Baumal *et al.*, 1998) though considering only 1 suspended seat implies that other seats are assumed to be fixed rigidly to the chassis. This assumption does not exactly match a physically real vehicle.

In general, the state-space form of a non-linear dynamic system can be written as follows:

$$\dot{\underline{x}} = \underline{f}(\underline{x}) + [B]\,\underline{u} \tag{1}$$

Here, $\underline{x} = [x_1 x_2 x_3 .... x_{16}]^T$ where $x_9 = \dot{x}_1$, $x_{10} = \dot{x}_2$ and so on. $\underline{f}(\underline{x})$ is vector functions composed of first order differential equations that can be non-linear, [B] is the controller coefficient matrix and $\underline{u} = [u_1 u_2 u_3 u_4 u_5]^T$ is the control input vector written for the most general case in this study. $\underline{f}(\underline{x})$ and [B] are given in the Appendix along with the nomenclature of vehicle parameters. Mathematically, u_1, u_2, u_3 and u_4 do not have to exist together. In order to control vehicle body motions, 3 controller forces are sufficient since the body has 3 degrees of

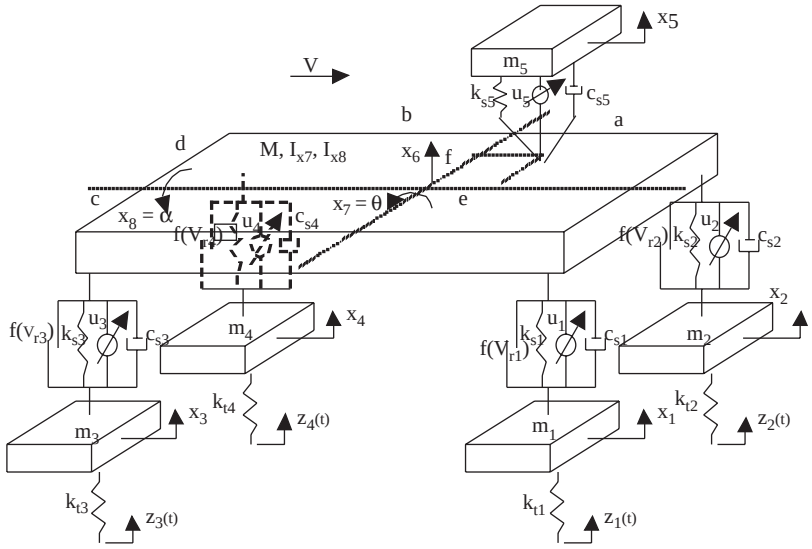

Figure 2. The non-linear full car model with a passenger seat.

freedom in this study. These are bounce, pitch and roll motions. But for practical reasons, 4 controllers parallel to the suspensions are introduced. The yaw motion is neglected. Finally, 5 controllers are used including the one under the passenger seat.

As mentioned before, the major non-linearity of the model comes from dry friction on the dampers. Geometric non-linearity has also been included. Dry friction on the dampers depends on the relative speed (V_r) between related damper ends. Experiments show that the dry friction model (Figure 3) has a viscous band character rather than being of a classical bang-bang type. The band ε is very small, and this prevents the complete locking of the suspension ends. Low speeds on perfect roads generate dry friction force around $\pm$R that practically (not ideally) locks the suspension generating a high equivalent viscous friction effect as introduced by Unlusoy and Yagiz (1986). The band ε only prevents ideal locking, as found by Yagiz (1986) after comparing his simulation results with a set of experimental ones obtained by Unlusoy (1979). The parameters are given in the Appendix.

PID Controller Design

The closed loop diagram of the feedback system is shown in Figure 4.

Here, $x_{ref}(t)$ is the desired value for the output of the system, x(t) is the output, e(t) is the error and u(t) is the control signal. PID control has been used widely and successfully in industry. The control input u(t) is obtained as follows:

$$u_i(t) = K[e_i(t) + \frac{1}{\tau_i}\int_0^t e_i(t)dt + \tau_d \frac{de_i(t)}{dt}] \quad (i = 1, 2, 3, 4, 5) \tag{2}$$

$$e_i(t) = x_{iref}(t) - x_i(t) \tag{3}$$

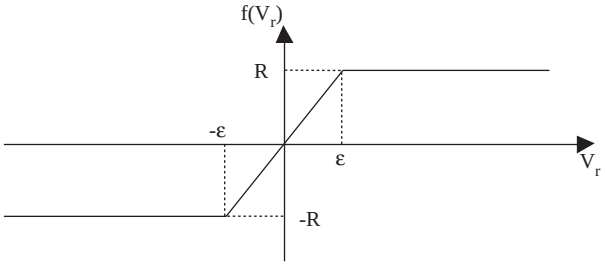

Figure 3. Dry friction model.

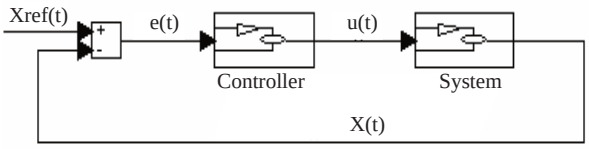

Figure 4. Closed loop block diagram with controller.

K, τ_i and τ_d are proportionality constant, integral time and derivative time, respectively. These values are obtained using the Ziegler-Nichols method (Ogata, 1990). In this method, should a unit change in reference value, using only a proportional controller, a proportionality constant of K_{mak} that results in continuous oscillatory motion in the system

is found. Then the period P_u of this oscillation is estimated. At the end, the PID parameters are decided as

$$K = 0.6 * K_{mak}, \quad \tau_i = P_u/2, \quad \tau_d = P_u/8 \qquad (4)$$

The vehicle model has been reduced to 1 degree of freedom equivalent systems for each degree of freedom having related natural frequencies and, by applying Ziegler-Nichols method, the PID constants are obtained. The errors are measured independently and the controllers are independent. The PID algorithm only allows the use of independent controllers. The related parameters for each controller are presented in the Appendix.

Simulation

In the simulation stage, first the non-linear model is used in order to obtain time responses. Second, for the frequency responses, the non-linear dry friction model is harmonically linearized using a describing function method. Accelerometers are used as sensors. These sensors are placed only to measure the states to be controlled. The data provided by these sensors are processed by micro-controllers having the PID algorithms designed. The noise is filtered using a low-pass filter, which allows the signals within the frequency range of the related vehicle dynamics.

Time response of the non-linear vehicle model

The vehicle is assumed to travel over the bump (Figure 5). The bump parameters are presented in the Appendix.

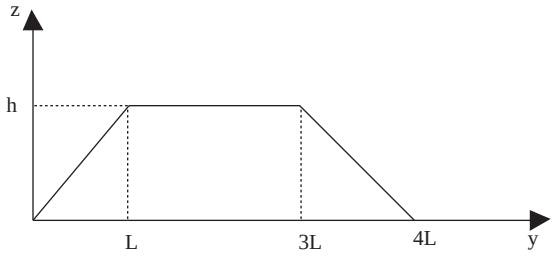

Figure 5. Road disturbance.

There is a time delay between the front and rear wheel inputs. This time delay is as follows:

$$\delta t = (a + b)/V \qquad (5)$$

where $(a + b)$ is the distance between the front and rear axles and V is the velocity of the vehicle. Vehicle body displacements for linear and non-linear models are presented for controlled and uncontrolled cases in Figure 6. It has been observed that the non-linear system is more damped due to the effect of dry friction.

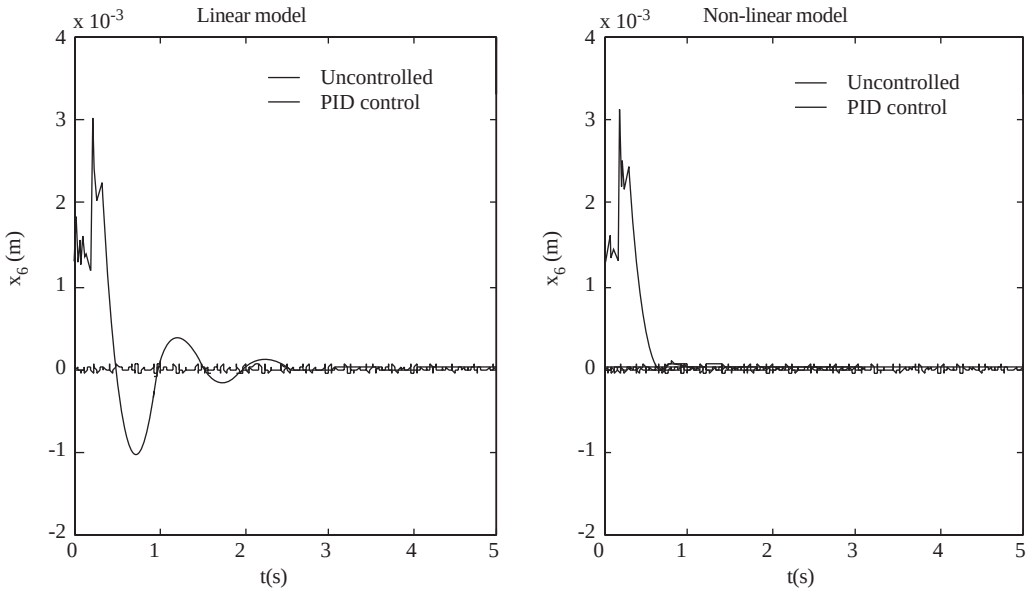

Figure 6. Vehicle body displacements for linear and non-linear models.

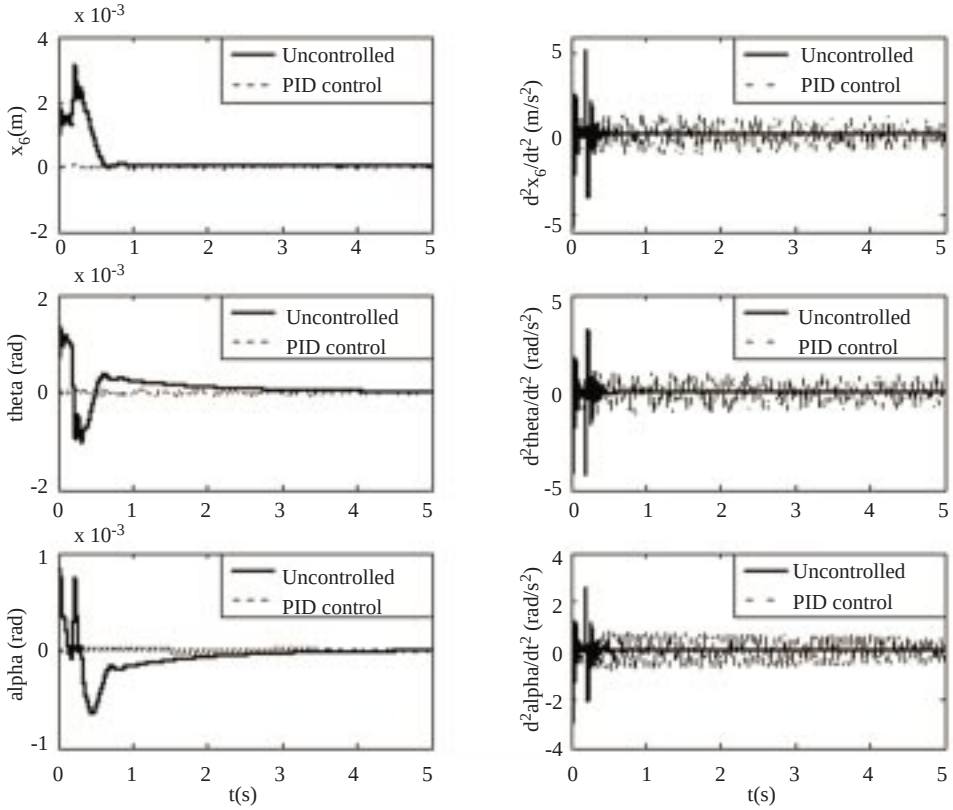

Figure 7. Time responses of the vehicle body displacement and its accelerations, pitch and roll angular displacement and their accelerations for controlled and uncontrolled cases for non-linear models.

The time responses of vehicle body displacement and its accelerations, sprung mass pitch and roll angular displacement and their accelerations and passenger seat displacements are shown in Figures 7 and 8 for controlled and uncontrolled cases for the non-linear model. The maximum displacement and accelerations of the active system are less than those of the passive system, and the active system returns to rest faster. As shown in Figure 8, the improvement obtained from the application of active suspensions for a passenger is clearly seen. For the third case, where the vehicle body and passenger seat are controlled together, the passenger is almost insensitive to the disturbance. This method, using selected strategy, is very effective. The vertical acceleration of the passenger is also an important criterion, which mainly affects ride comfort since the force generated by the inertia of the passenger creates disturbances. In other words, minimizing the vertical displacement may not mean an improvement in itself alone, as an improvement in the acceleration is also obtained.

In Figure 9, the acceleration of the passenger in different cases of the non-linear model is shown. The PID controller decreases the amplitude of the acceleration in all 3 cases when compared with the uncontrolled example. The most suitable strategy is, therefore, the third one.

Another criterion is the control forces used since it is directly related with the cost of the controller. Figure 10 shows the controller force inputs for the selected strategies. In the first case, using a maximum control force of 60 N can damp the passenger's vertical displacement. However, no comment can be made for the angular displacement of the passenger in this case. In the third case, the front and rear suspensions apply a maximum force of about 5000 N. The amount of force applied to the passenger seat decreases since the body is controlled and the passenger seat is slightly isolated. A 3 N maximum force is sufficient to bring the passenger to the reference value of zero displacement. In simulation, a saturation value of $\pm$ 100 N for the linear motor of the passenger seat and a saturation value of $\pm$ 10000 N for the suspension linear motors was used.

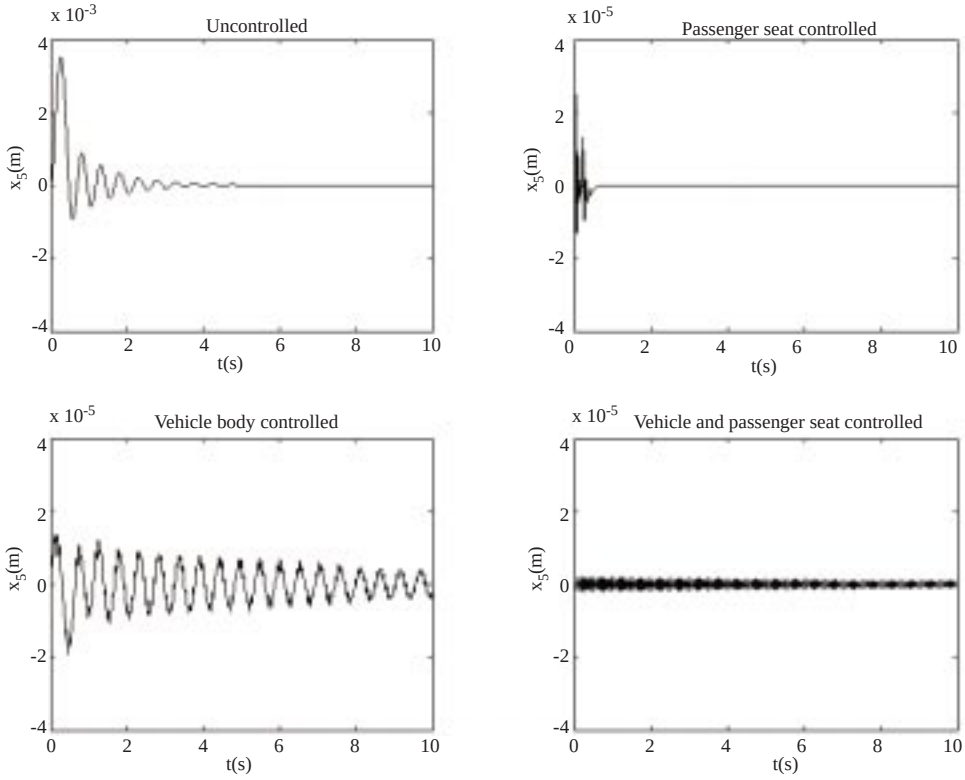

Figure 8. Time responses of passenger displacement for the non-linear model.

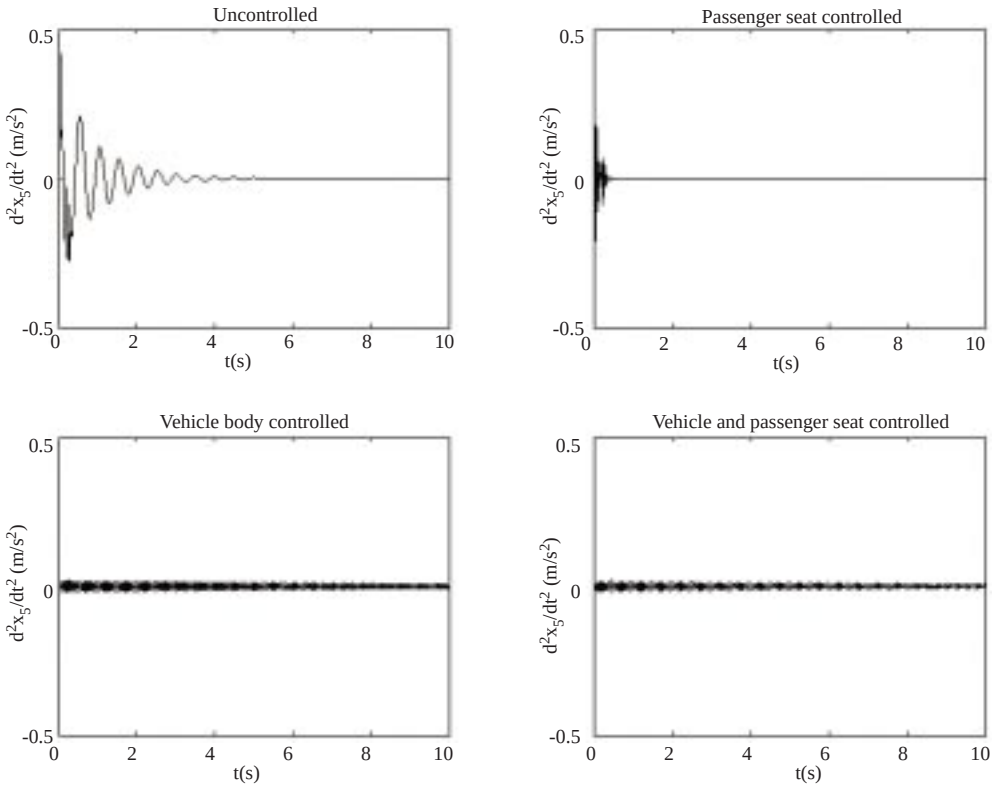

Figure 9. Time responses of passenger vertical acceleration for the non-linear model.

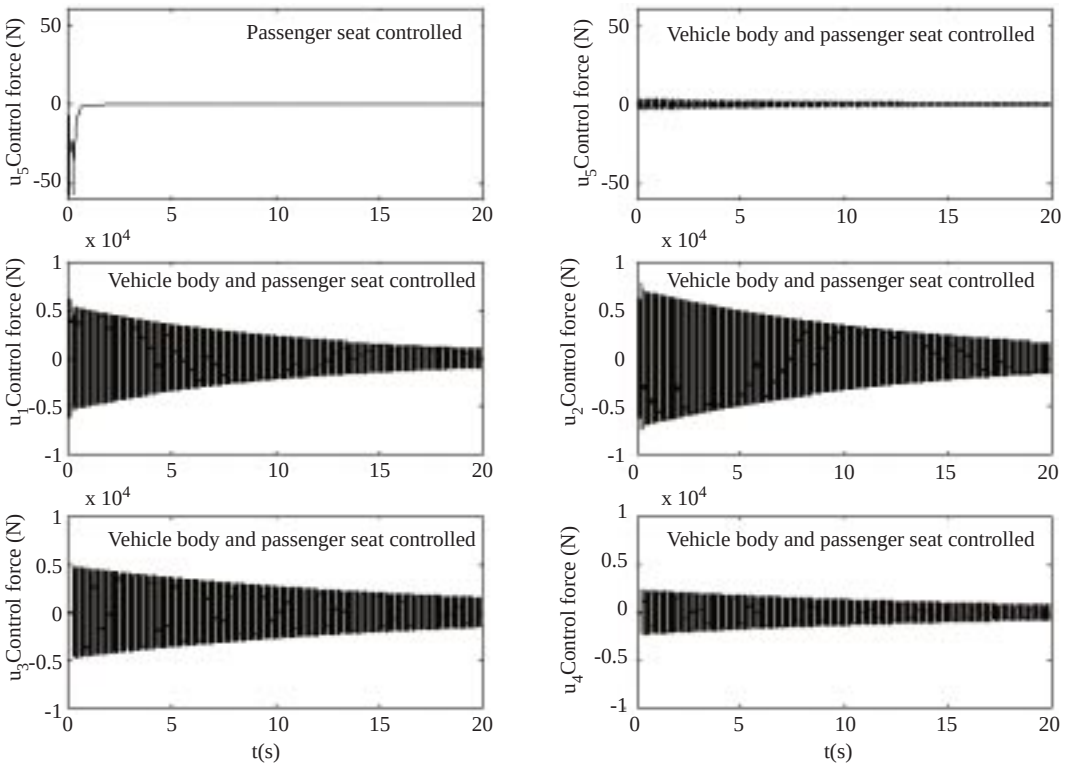

Figure 10. Control force inputs for various strategies.

Frequency response of the vehicle model

Frequency response is another key to understand the behavior of a dynamic system. Frequency response analysis is the main tool in interpreting the dynamic behavior of vehicles. Since the frequency response plot of a non-linear system is dependent on input and is not unique (there are infinite response plots for infinite inputs), the dry friction model is harmonically linearized in frequency response analysis whereas non-linear ones were used in time response analysis. Linearization without ignoring non-linearity is achieved by using the describing function method for dry friction on dampers as developed by Yagiz (1986) and assuming that the vehicle body angular motions are small. In this technique, the effect of a non-linear dry friction model is replaced by a linear equivalent damping coefficient (C_e) obtained by the describing function method.

$$C_e = \frac{1}{\pi.V_{ro}} \int_0^{2.\pi} f(V_r).Sin\omega.t.d(\omega t) \qquad (6)$$

The sinusoidal response of non-linearity is given in Figure 11, where relative velocity is given by

$$V_r(t) = V_{ro}.Sin\omega.t \qquad (7)$$

the dry friction force is

$$f(V_r) = \begin{cases} +R & V_r \geq \varepsilon \\ n.V_r & -\varepsilon < V_r < \varepsilon \\ -R & V_r \leq \varepsilon \end{cases} \qquad (8)$$

Let $\omega.t = \theta$ when $V_r = \varepsilon$. Then Eq. (7) becomes

$$\varepsilon = V_{ro}.Sin\theta \qquad (9)$$

and

$$\theta = Sin^{-1}\left(\frac{\varepsilon}{V_{ro}}\right) \qquad (10)$$

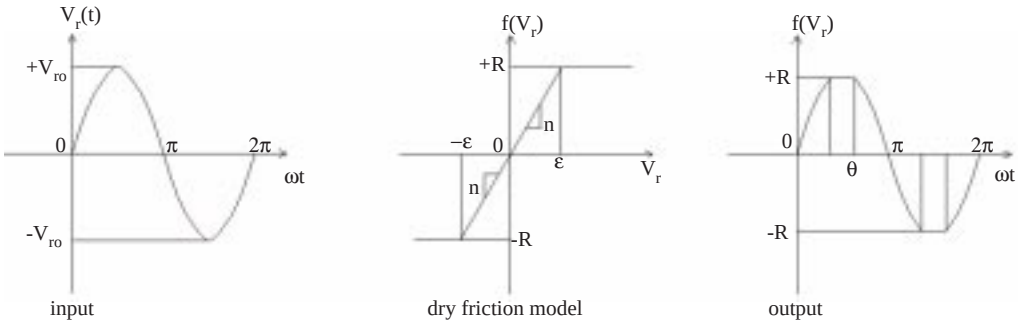

Figure 11. Sinusoidal response of a dry friction model.

The output is again symmetrical at about $\pi/2$ (Figure 11) and Eq. (6) can be rearranged using Eq. (8) as below:

$$C_e = \frac{4}{\pi.V_{ro}} \int_0^{\theta} (n.V_r) \,.Sin\omega t.d\,(\omega t) + \frac{4}{\pi.V_{ro}} \int_{\theta}^{\pi/2} RSin\omega t.d\,(\omega t) \tag{11}$$

The integration of Eq. (11) gives the following formulation known as the expression for the equivalent damping coefficient:

$$C_e = \frac{n}{\pi}\,(2.\theta - Sin2.\theta) + \frac{4.R}{\pi.V_{ro}} Cos\theta \tag{12}$$

If $V_{ro} < \varepsilon$ then dry friction is represented by a viscous band of slope n. Therefore,

$$C_e = n \tag{13}$$

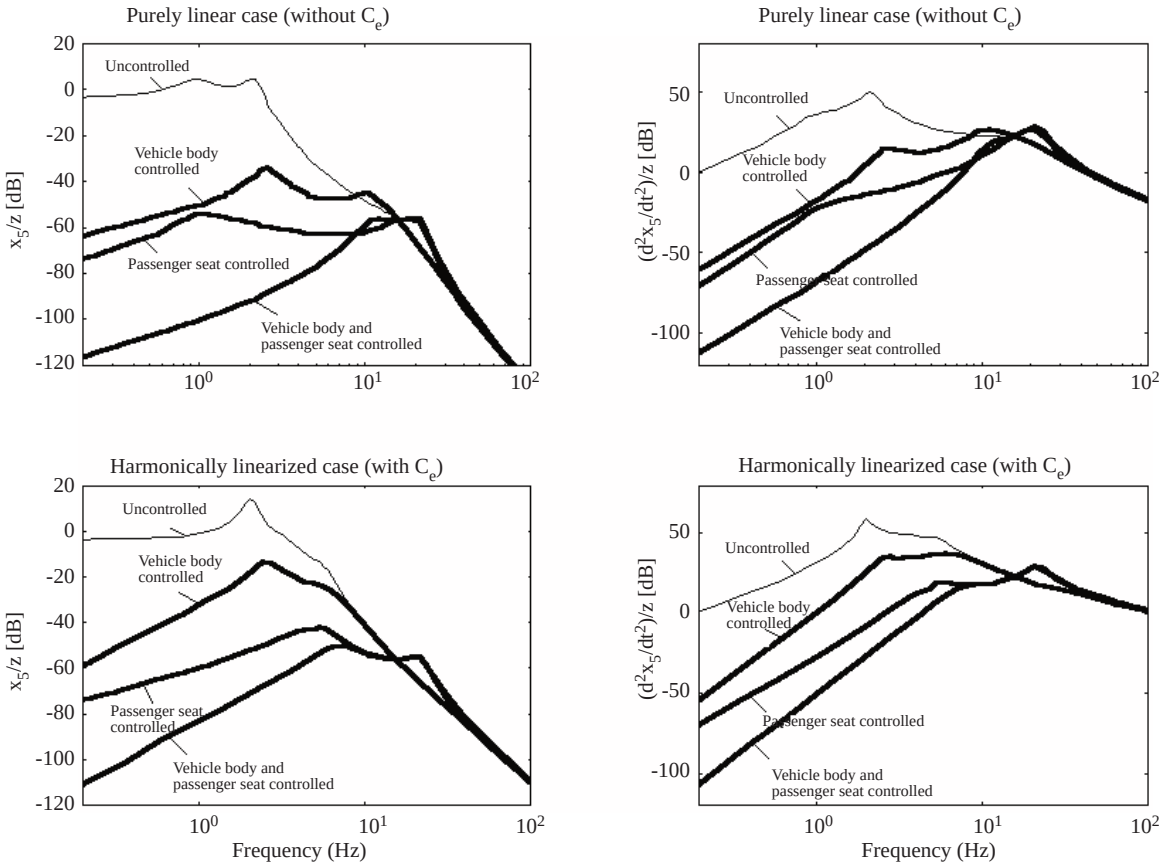

Figure 12. Frequency response plots of passenger displacements and accelerations.

In Figure 12, the frequency response plots of the passenger seat displacements and accelerations for all strategies are considered for both those with C_e and those without C_e in order to observe the difference between the purely linear and harmonically linearized non-linear cases. When the frequency response plots of an uncontrolled passenger seat for purely linear and harmonically linearized cases are compared, a new natural frequency around 2 Hz is observed as a damper locking effect including the dry friction. Three visual groups of resonance frequencies in the uncontrolled case are observed in logarithmic plots. These belong to vehicle body motions, the passenger and unsprung masses, respectively. Actually, the linear vehicle model has 8 resonance frequencies. The values of related natural frequencies are obtained by solving the eigenvalue problem using Matlab. These values are 0.975, 1.183, 1.396, 2.202, 12.261, 12.264, 16.387 and 16.388 Hz, respectively. In all control strategies, the amplitudes of resonance frequencies of almost all degrees of freedom decrease, the only exception being in unsprung mass resonances. The overall magnitudes also decrease in the controlled cases. The improvement observed in the unsprung mass resonance frequencies is not very effective as in the other examples. The reason for this is that the controllers only work on the vehicle body and the passenger seat. The third case gives the maximum displacement and acceleration isolation for the passenger as shown in the figures. As seen in Figure 12, the best improvement in terms of ride comfort is obtained when both the vehicle body and passenger seat are under control action.

Conclusion

The main idea behind proposing this controller is the ability to use these types of controllers on vehicles with developing technology. PID control, which is easy to design and has good performance, has been applied. The simulation results prove that, among 3 control strategies considered, using controllers under the vehicle body and passenger seat will provide the best ride comfort. The first case, only having a controller under the passenger seat, cannot guarantee ride comfort since it does not have control over the angular motions of the vehicle or the passenger. The second case, where only the vehicle body is under control, provides sufficient vehicle motions, but it does not provide good control over passenger comfort. Therefore, the third strategy should be taken into account by considering the control of the vehicle body and passenger seat together. Using the third strategy, the bounce motion of the passenger almost vanishes with an extra controller that applies very small force input. A successful improvement has also been obtained in the isolation of the vertical acceleration of passengers. Frequency response plots of a passenger for these alternatives support the results obtained. When frequency responses of the passenger seat for linear and non-linear models are compared for controlled and uncontrolled cases, the damper locking effect of dry friction is also observed. In conclusion, adding a controller under the passenger seat improves ride comfort greatly.

Nomenclature

a, b	distances of axle to the center of gravity of the vehicle body
c, d	distances of unsprung masses to the center of gravity of the axles
e, f	distances of passenger seat to the center of gravity of the vehicle body
c_{si}	i^{th} damping coefficient of suspension
c_{s5}	damping coefficient of passenger seat
e(t)	error
$f(V_{ri})$	i^{th} dry friction force
k_{si}	i^{th} spring constant of suspension
k_{s5}	spring constant of passenger seat
k_{ti}	i^{th} stiffness coefficient of tire
m_1	i^{th} mass of axle
m_5	mass of the passenger
u(t)	control signal
x(t)	output
$x_{ref}(t)$	desired value
x_i	i^{th} state variable
$z_i(t)$	i^{th} road excitation
I_{x7}	mass moment of inertia of the vehicle body for pitch motion
I_{x8}	mass moment of inertia of the vehicle body for roll motion
K	proportionality constant
M	mass of the vehicle body
τ_d	derivative time
τ_i	integral time

References

Alleyne, A., Neuhaus, P.D. and Hedrick, J.K., "Application of Non-linear Control Theory to Electronically Controlled Suspensions", Vehicle System Dynamics, 22, 309-320, 1993.

Baumal, A.E., McPhee, J.J. and Calamai, P.H., "Application of Genetic Algorithms to the Design Optimization of an Active Vehicle Suspension System", Computer Methods in Applied Mechanics and Engineering, 163, 87-94, 1998.

Crolla, D.A. and Abdel Hady, M.B.A., "Active Suspension Control; Performance Comparisons Using Control Laws Applied to a Full Car Model", Vehicle System Dynamics, 20, 107-120, 1991.

Hac, A., "Optimal Linear Preview Control of Active Vehicle Suspension", Vehicle System Dynamics, 21, 167-195, 1992.

Hrovat, D., "Applications of Optimal Control to Advanced Automotive Suspension Design", Journal of Dynamic Systems, Measurement, and Control, 115, 328-342, 1993.

Ogata, K., Modern Control Engineering, Prentice-Hall, New Jersey, 1990.

Otten, G., de Vries, T.J.A., Rankers, A.M. and Gaal, E.W., "Linear Motor Motion Control Using a Learning Feedforward Controller", IEEE/ASME Transactions on Mechatronics, 2(3), September, 1997.

Rakheja, S., Afework, Y. and Sankar, S., "An Analytical and Experimental Investigation of the Driver-Seat-Suspension System", Vehicle System Dynamics, 23, 501-524, 1994.

Redfield, R.C. and Karnopp, D.C., "Optimal Performance of Variable Component Suspensions" , Vehicle System Dynamics, 17, 231-253, 1988.

Silvester, B.C., "Vibration Reduction in Motor Cars", Soc. Environmental Engineers, 4, 1966.

Stein, G.J. and Ballo, I., "Active Vibration Control System for the Driver's Seat for Off-Road Vehicles", Vehicle System Dynamics, 20, 57-78, 1991.

Unlusoy, Y.S., "Suspension System Dynamics and Vehicle Noise Control", PhD Thesis, University of Birmingham, 1979.

Unlusoy, Y.S. and Yagiz, N., "Simulation of the Effects of Dry Friction on Suspension Dynamics and Vehicle Ride", Int. AMSE Conference, Sorrento, Italy, September 29-October 1, 1986.

Yagiz, N., "Effects of Dry Friction on Suspension Dynamics and Vehicle Ride", MSc Thesis, Mechanical Engineering Department, METU, 1986.

Yagiz, N., Yuksek, I. and Sivrioglu, S., "Robust Control of Active Suspensions for a Full Vehicle Model Using Sliding Mode Control", JSME International Journal, 43, 253-258, 2000.

Yue, C., Butsuen, T. and Hedrick, J.K., "Alternative Control Laws for Automotive Active Suspensions", Journal of Dynamic Systems, Measurement and Control, 111, 286-291, 1989.

Appendix

The parameters of the vehicle:

M = 1100 kg, I_{x7}= 1848 kg.m^2, I_{x8}= 550 kg.m^2

m_1= m_2= 25 kg, m_3= m_4= 45 kg, m_5= 90 kg

$k_{s1} = k_{s2}$ = 15000 N/m, $k_{s3} = k_{s4}$ = 17000 N/m, k_{s5} = 15000 N/m

c_{s1}= c_{s2} = c_{s3}= c_{s4} = 2500 N.s/m, c_{s5} = 150 N.s/m

$k_{t1} = k_{t2} = k_{t3} = k_{t4}$ = 250000 N/m

a = 1.2 m, b = 1.4 m, c = 0.5 m, d = 1.0 m, e = 0.3 m, f = 0.25 m

The parameters of the road bump:

h = 0.035 m, L = 0.025 m

Dry friction parameters:

R = 22 N, $\varepsilon = 0.0012$ m/s

State equations excluding control inputs:

$f_1(x) = x_9, \quad f_2(x) = x_{10}, \quad f_3(x) = x_{11}, \quad f_4(x) = x_{12}$

$f_5(x) = x_{13}, \quad f_6(x) = x_{14}, \quad f_7(x) = x_{15}, \quad f_8(x) = x_{16}$

$$f_9(x) = 1/m_1\{-(k_{s1}+k_{t1})\,x_1 + k_{s1}\,x_6 + a\,k_{s1}\,Sin\,x_7 - c\,k_{s1}\,Sin\,x_8 - c_{s1}\,x_9 + c_{s1}\,x_{14}$$
$$+a\,c_{s1}Cosx_7\,x_{15} - c\,c_{s1}\,Cos\,x_8\,x_{16} + k_{t1}\,z_1 + f\,(V_{r1})\}$$

$$f_{10}(x) = 1/m_2\{-(k_{s2}+k_{t2})\,x_2 + k_{s2}\,x_6 + a\,k_{s2}\,Sin\,x_7 + d\,k_{s2}\,Sin\,x_8 - c_{s2}\,x_{10} + c_{s2}\,x_{14}$$
$$+a\,c_{s2}Cosx_7\,x_{15} + d\,c_{s2}\,Cos\,x_8\,x_{16} + k_{t2}\,z_2 + f\,(V_{r2})\}$$

$$f_{11}(x) = 1/m_3\{-(k_{s3}+k_{t3})\,x_3 + k_{s3}\,x_6 - b\,k_{s3}\,Sin\,x_7 - c\,k_{s3}\,Sin\,x_8 - c_{s3}\,x_{11} + c_{s3}\,x_{14}$$
$$-b\,c_{s3}Cosx_7\,x_{15} - c\,c_{s3}\,Cos\,x_8\,x_{16} + k_{t3}\,z_3 + f\,(V_{r3})\}$$

$$f_{12}(x) = 1/m_4\{-(k_{s4}+k_{t4})\,x_4 + k_{s4}\,x_6 - b\,k_{s4}\,Sin\,x_7 + d\,k_{s4}\,Sin\,x_8 - c_{s4}\,x_{12} + c_{s4}\,x_{14}$$
$$-b\,c_{s4}Cosx_7\,x_{15} + d\,c_{s4}\,Cos\,x_8\,x_{16} + k_{t4}\,z_4 + f\,(V_{r4})\}$$

$$f_{13}(x) = 1/m_5\{-k_{s5}\,x_5 + k_{s5}\,x_6 + e\,k_{s5}\,Sin\,x_7 + f\,k_{s5}\,Sin\,x_8 - c_{s5}\,x_{14} + c_{s5}\,x_{14}$$
$$+e\,c_{s5}Cosx_7\,x_{15} + f\,c_{s5}\,Cos\,x_8\,x_{16}\}$$

$$f_{14}(x) = 1/M\{k_{s1}\,x_1 + k_{s2}\,x_2 + k_{s3}\,x_3 + k_{s4}\,x_4 + k_{s5}\,x_5 - (k_{s1}+k_{s2}+k_{s3}+k_{s4}+k_{s5})\,x_6$$
$$-(a\,(k_{s1}+k_{s2}) - b\,(k_{s3}+k_{s4}) + e\,k_{s5})\,Sin\,x_7 - (d\,(k_{s2}+k_{s4}) - c\,(k_{s1}+k_{s3}) + f\,k_{s5})\,Sin\,x_8$$
$$+c_{s1}\,x_9 + c_{s2}\,x_{10} + c_{s3}\,x_{11} + c_{s4}\,x_{12} + c_{s5}\,x_{13} - (c_{s1}+c_{s2}+c_{s3}+c_{s4}+c_{s5})\,x_{14}$$
$$-(a\,(c_{s1}+c_{s2}) - b\,(c_{s3}+c_{s4}) + e\,c_{s5})\,Cos\,x_7x_{15} - (d\,(c_{s2}+c_{s4}) - c\,(c_{s1}+c_{s3}) + f\,c_{s5})\,Cos\,x_8\,x_{16}$$
$$-f\,(V_{r1}) - f\,(V_{r2}) - f\,(V_{r3}) - f\,(V_{r4})\}$$

$$f_{15}(x) = 1/I_{x7}\{a\,k_{s1}\,x_1 + a\,k_{s2}\,x_2 - b\,k_{s3}\,x_3 - b\,k_{s4}\,x_4 + e\,k_{s5}\,x_5 - (a\,(k_{s1}+k_{s2}) - b\,(k_{s3}+k_{s4}) + e\,k_{s5})\,x_6$$
$$-\left(a^2\,(k_{s1}+k_{s2}) + b^2\,(k_{s3}+k_{s4}) + e^2k_{s5}\right)\,Sinx_7 - (d\,(a\,k_{s2} - b\,k_{s4}) - c\,(a\,k_{s1} - b\,k_{s3}) + e\,f\,k_{s5})Sinx_8$$
$$+a\,c_{s1}\,x_9 + a\,c_{s2}\,x_{10} - b\,c_{s3}\,x_{11} - b\,c_{s4}\,x_{12} + e\,c_{s5}\,x_{13} - (a\,(c_{s1}+c_{s2}) - b\,(c_{s3}+c_{s4}) + e\,c_{s5})\,x_{14}$$
$$-\left(a^2\,(c_{s1}+c_{s2}) + b^2\,(c_{s3}+c_{s4}) + e^2c_{s5}\right)\,Cosx_7x_{15} - (d\,(a\,c_{s2} - b\,c_{s4}) - c\,(a\,c_{s1} - b\,c_{s3}) + e\,f\,c_{s5})Cosx_8x_{16}$$
$$-a\,f\,(V_{r1}) - a\,f\,(V_{r2}) + b\,f\,(V_{r3}) + b\,f\,(V_{r4})\}Cos\,x_7$$

$$f_{16}(x) = 1/I_{x8}\{-c\,k_{s1}\,x_1 + d\,k_{s2}\,x_2 - c\,k_{s3}\,x_3 + d\,k_{s4}\,x_4 + f\,k_{s5}\,x_5 - (d\,(k_{s2}+k_{s4}) - c\,(k_{s1}+k_{s3}) + f\,k_{s5})\;x_6$$
$$-(d\,(a\,k_{s2} - b\,k_{s4}) - c\;(a\,k_{s1} - b\,k_{s3}) + e\,f\,k_{s5})\,Sinx_7 - (d^2(k_{s2}+k_{s4}) + c^2\,(k_{s1}+k_{s3}) + f^2 k_{s5})Sinx_8$$
$$-c\,c_{s1}\,x_9 + d\,c_{s2}\,x_{10} - c\,c_{s3}\,x_{11} + d\,c_{s4}\,x_{12} + f\,c_{s5}\,x_{13} - (d\,(c_{s2}+c_{s4}) - c\,(c_{s1}+c_{s3}) + f\,c_{s5})\;x_{14}$$
$$-(d\,(a\,c_{s2} - b\,c_{s4}) - c\;(a\,c_{s1} - b\,c_{s3}) + e\,f\,c_{s5})\,Cos\,x_7 x_{15} - (d^2(c_{s2}+c_{s4}) + c^2(c_{s1}+c_{s3}) + f^2 c_{s5})Cos\,x_8 x_{16}$$
$$-c\;f\,(V_{r1}) + d\,f\,(V_{r2}) - c\,f\,(V_{r3}) + d\,f\,(V_{r4})\}Cos\,x_8$$

f $(\mathrm{Vr}_i) = \mathrm{Ce}_i(\dot{y}_i - \dot{x}_i)$ (i = 1, 2, 3, 4)

$y_1 = x_6 + a\,Sinx_7 - c\,Sinx_8$

$y_2 = x_6 + a\,Sin\,x_7 + d\,Sin\,x_8$

$y_3 = x_6 - b\,Sin\,x_7 - c\,Sin\,x_8$

$y_4 = x_6 - b\,Sin\,x_7 + d\,Sin\,x_8$

$$Ce_i = \begin{cases} n\;if\left|\dot{y}_i - \dot{x}_i\right| < \varepsilon \\ \\ \frac{n}{\pi}(2\theta_i - Sin2\theta_i) + \frac{4R}{\pi\left|\dot{y}_i - \dot{x}_i\right|}Cos\theta_i \quad else \end{cases} \qquad \text{where } \theta_i = Sin^{-1}\frac{\varepsilon}{\left|\dot{y}_i - \dot{x}_i\right|}$$

The controller force matrix:

$$[B] = \begin{bmatrix} 0 & 0 & 0 & 0 \\ 0 & 0 & 0 & 0 \\ 0 & 0 & 0 & 0 \\ 0 & 0 & 0 & 0 \\ 0 & 0 & 0 & 0 \\ 0 & 0 & 0 & 0 \\ 0 & 0 & 0 & 0 \\ 0 & 0 & 0 & 0 \\ -\frac{b\,d}{(a+b)\,(c+d)\,m_1} & -\frac{d}{(a+b)\,(c+d)m_1} & \frac{1}{(c+d)\,m_1} & \frac{-d(b+e)+f(a+b)}{(a+b)\,(c+d)\,m_1} \\ -\frac{b\,c}{(a+b)\,(c+d)\,m_2} & -\frac{c}{(a+b)\,(c+d)\,m_2} & -\frac{1}{(c+d)\,m_2} & \frac{-c(b+e)-f(a+b)}{(a+b)\,(c+d)\,m_2} \\ -\frac{a\,d}{(a+b)\,(c+d)\,m_3} & \frac{d}{(a+b)\,(c+d)\,m_3} & 0 & -\frac{d\,(a-e)}{(a+b)\,(c+d)\,m_3} \\ -\frac{a\,c}{(a+b)\,(c+d)\,m_4} & \frac{c}{(a+b)\,(c+d)\,m_4} & 0 & -\frac{c\,(a-e)}{(a+b)\,(c+d)\,m_4} \\ 0 & 0 & 0 & \frac{1}{m_5} \\ \frac{1}{M} & 0 & 0 & 0 \\ 0 & \frac{1}{I_{x7}} & 0 & 0 \\ 0 & 0 & \frac{1}{I_{x8}} & 0 \end{bmatrix}$$

Controller parameters for vehicle body bounce:

$\mathrm{K}_{mak1} = 11 \times 10^6$ N/m, $\mathrm{K}_1 = 6.6 \times 10^6$ N/m

$\mathrm{Pu}_1 = 3.5$ s, $\tau_{i1} = 1.75$ s, $\tau_{d1} = 0.4375$ s

Controller parameters for vehicle body pitch:

$K_{mak2} = 23 \times 10^6$ Nm/rad, $K_2 = 13.8 \times 10^6$ Nm/rad

Pu_2= 2.3 s, τ_{i2}= 1.15 s, τ_{d2}= 0.2875 s

Controller parameters for vehicle body roll:

$K_{mak3} = 12 \times 10^6$ Nm/rad, $K_3 = 7.2 \times 10^6$ Nm/rad

Pu_3 = 1.5 s, τ_{i3}= 0.75 s, τ_{d3}= 0.1875 s

Controller parameters for passenger seat:

$K_{mak4} = 25 \times 10^5$ N/m, $K_4 = 15 \times 10^5$ N/m

Pu_4= 0.05 s, τ_{i4}= 0.025 s, τ_{d4}= 0.00625 s